

University of Groningen

Non-canonical PRC1.1 Targets Active Genes Independent of H3K27me3 and Is Essential for Leukemogenesis

van den Boom, Vincent; Maat, Henny; Geugien, Marjan; Lopez, Aida Rodriguez; Sotoca, Ana M.; Jaques, Jennifer; Brouwers-Vos, Annet Z.; Fusetti, Fabrizia; Groen, Richard W. J.; Yuan, Huipin

Published in:
Cell reports

DOI:
[10.1016/j.celrep.2015.12.034](https://doi.org/10.1016/j.celrep.2015.12.034)

IMPORTANT NOTE: You are advised to consult the publisher's version (publisher's PDF) if you wish to cite from it. Please check the document version below.

Document Version
Publisher's PDF, also known as Version of record

Publication date:
2016

[Link to publication in University of Groningen/UMCG research database](#)

Citation for published version (APA):

van den Boom, V., Maat, H., Geugien, M., Lopez, A. R., Sotoca, A. M., Jaques, J., Brouwers-Vos, A. Z., Fusetti, F., Groen, R. W. J., Yuan, H., Martens, A. C. M., Stunnenberg, H. G., Vellenga, E., Martens, J. H. A., & Schuringa, J. J. (2016). Non-canonical PRC1.1 Targets Active Genes Independent of H3K27me3 and Is Essential for Leukemogenesis. *Cell reports*, 14(2), 332-346. <https://doi.org/10.1016/j.celrep.2015.12.034>

Copyright

Other than for strictly personal use, it is not permitted to download or to forward/distribute the text or part of it without the consent of the author(s) and/or copyright holder(s), unless the work is under an open content license (like Creative Commons).

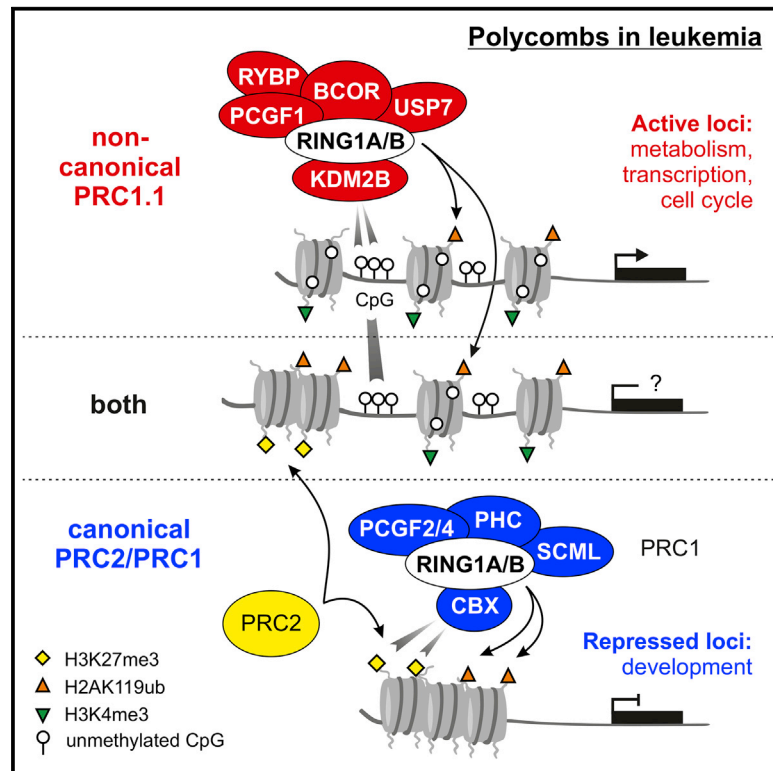
The publication may also be distributed here under the terms of Article 25fa of the Dutch Copyright Act, indicated by the "Taverne" license. More information can be found on the University of Groningen website: <https://www.rug.nl/library/open-access/self-archiving-pure/taverne-amendment>.

Take-down policy

If you believe that this document breaches copyright please contact us providing details, and we will remove access to the work immediately and investigate your claim.

Non-canonical PRC1.1 Targets Active Genes Independent of H3K27me3 and Is Essential for Leukemogenesis

Graphical Abstract



Authors

Vincent van den Boom, Henny Maat, Marjan Geugien, ..., Edo Vellenga, Joost H.A. Martens, Jan Jacob Schuringa

Correspondence

j.j.schuringa@umcg.nl

In Brief

Polycomb proteins regulate stem cell self-renewal and are frequently deregulated in cancer. Van den Boom et al. show that PRC1.1, a non-canonical Polycomb complex, is essential for primary leukemic stem cells in vitro and in humanized xenograft models. PRC1.1 targets active genes involved in metabolism, independent of PRC2.

Highlights

- The non-canonical PRC1.1 complex is critically important for human LSCs
- Several PRC1.1 members are overexpressed in primary human AML
- PRC1.1 can bind TSSs in the absence of the repressive H3K27me3 PRC2 mark
- PRC1.1 targets actively transcribed genes involved in metabolism

Accession Numbers

GSE54580



Non-canonical PRC1.1 Targets Active Genes Independent of H3K27me3 and Is Essential for Leukemogenesis

Vincent van den Boom,^{1,7} Henny Maat,^{1,7} Marjan Geugien,^{1,2} Aida Rodríguez López,¹ Ana M. Sotoca,³ Jennifer Jaques,¹ Annet Z. Brouwers-Vos,¹ Fabrizia Fusetti,⁴ Richard W.J. Groen,⁵ Huipin Yuan,⁶ Anton C.M. Martens,⁵ Hendrik G. Stunnenberg,³ Edo Vellenga,¹ Joost H.A. Martens,³ and Jan Jacob Schuringa^{1,*}

¹Department of Experimental Hematology, Cancer Research Center Groningen, University Medical Center Groningen, University of Groningen, Hanzeplein 1, 9700RB Groningen, the Netherlands

²Department of Laboratory Medicine, University Medical Center Groningen, University of Groningen, Hanzeplein 1, 9700RB Groningen, the Netherlands

³Department of Molecular Biology, Radboud Institute for Molecular Life Sciences, Radboud University Nijmegen, Geert Grooteplein 28, 6525 GA Nijmegen, the Netherlands

⁴Department of Biochemistry, Groningen Biomolecular Sciences and Biotechnology Institute, Netherlands Proteomics Centre and Zernike Institute for Advanced Materials, University of Groningen, Nijenborgh 4, 9747 AG, Groningen, the Netherlands

⁵Department of Hematology, VU University Medical Center Amsterdam, De Boelelaan 1117, 1081 HV Amsterdam, the Netherlands

⁶Xpand Biotechnology BV, Professor Bronkhorstlaan 10, 3723 MB Bilthoven, the Netherlands

⁷Co-first author

*Correspondence: j.j.schuringa@umcg.nl

<http://dx.doi.org/10.1016/j.celrep.2015.12.034>

This is an open access article under the CC BY-NC-ND license (<http://creativecommons.org/licenses/by-nc-nd/4.0/>).

SUMMARY

Polycomb proteins are classical regulators of stem cell self-renewal and cell lineage commitment and are frequently deregulated in cancer. Here, we find that the non-canonical PRC1.1 complex, as identified by mass-spectrometry-based proteomics, is critically important for human leukemic stem cells. Downmodulation of PRC1.1 complex members, like the DNA-binding subunit KDM2B, strongly reduces cell proliferation *in vitro* and delays or even abrogates leukemogenesis *in vivo* in humanized xenograft models. PRC1.1 components are significantly overexpressed in primary AML CD34⁺ cells. Besides a set of genes that is targeted by PRC1 and PRC2, ChIP-seq studies show that PRC1.1 also binds a distinct set of genes that are devoid of H3K27me3, suggesting a gene-regulatory role independent of PRC2. This set encompasses genes involved in metabolism, which have transcriptionally active chromatin profiles. These data indicate that PRC1.1 controls specific genes involved in unique cell biological processes required for leukemic cell viability.

INTRODUCTION

Stem cell self-renewal and lineage specification are tightly regulated processes that are of vital importance for proper embryonic development and maintenance of somatic stem cells in adults. The Polycomb group protein family of epigenetic modifiers is

critically involved in the regulation of stem cell self-renewal and differentiation.

In general, Polycomb proteins reside in two complexes: the Polycomb repressive complex 1 (PRC1) and 2 (PRC2) (Simon and Kingston, 2013). The PRC2 complex, consisting of the core components EED, SUZ12, and EZH1 or EZH2, can trimethylate lysine 27 on histone H3 (H3K27me3) via EZH1 or EZH2 (Cao et al., 2002; Ezhkova et al., 2011; Kirmizis et al., 2004; Kuzmichev et al., 2002; Shen et al., 2008). The PRC1 complex has five subunits (PCGF, PHC, CBX, SCM, and RING1) and displays RING1-mediated ubiquitination activity toward histone H2A at lysine 119 (H2AK119ub) (Buchwald et al., 2006; de Napoles et al., 2004; Levine et al., 2002; Wang et al., 2004). The human genome encodes for multiple paralogs for each of the PRC1 subunits: six PCGF members (PCGF1, PCGF2, PCGF3, PCGF4, PCGF5, and PCGF6), three PHC members (PHC1, PHC2, and PHC3), five CBX members (CBX2, CBX4, CBX6, CBX7, and CBX8), three SCM members (SCML1, SCML2, and SCMH1), and two RING1 members (RING1A and RING1B). Accumulating evidence suggests that PRC1 paralogs reside in the complex in a mutually exclusive manner, allowing a so-far poorly understood complexity of regulation by PRC1 (Gao et al., 2012; Maertens et al., 2009; Morey et al., 2012; van den Boom et al., 2013; Vandamme et al., 2011).

The classical view on Polycomb-mediated silencing is a consecutive model where PRC2 first trimethylates H3K27 followed by CBX-dependent binding of PRC1 to H3K27me3 and subsequent ubiquitination of H2AK119 (Cao et al., 2002; Bernstein et al., 2006; Kaustov et al., 2011). In line with this model, genome-wide chromatin binding studies showed frequent co-occupancy of PRC1 and PRC2 at Polycomb target genes in mammalian cells (Boyer et al., 2006; Bracken et al., 2006; Lee

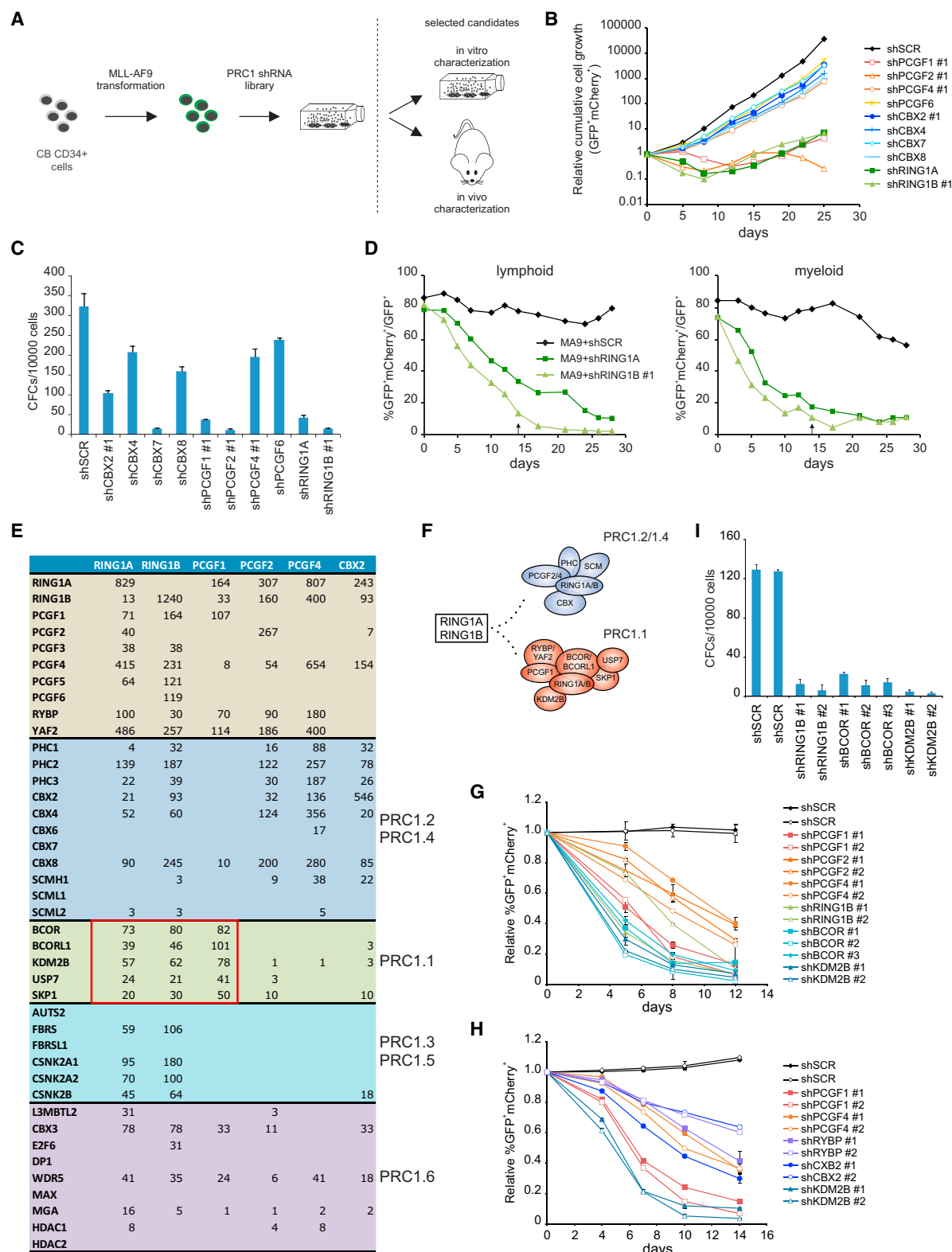


Figure 1. Primary MLL-AF9 Leukemic Cells Critically Depend on PRC1.1

(A) Schematic overview of a Polycomb shRNA screen in primary MLL-AF9 (MA9)-transformed CB cells.
(B) Cumulative cell growth of MA9 cells in a sorted liquid culture expressing indicated Polycomb shRNAs.

(legend continued on next page)

et al., 2006). PRC1 complexes containing a CBX subunit and PCGF2 (MEL18) or PCGF4 (BMI1) are referred to as canonical PRC1 complexes (PRC1.2/PRC1.4) and often co-occupy target loci (Gao et al., 2012). However, recent work from various groups led to the identification of a class of non-canonical PRC1 complexes that contain RYBP but lack a CBX subunit and are targeted to chromatin independently of H3K27me3 (Morey et al., 2013; Tavares et al., 2012). In addition, other non-canonical PRC1 complexes were identified that are targeted to chromatin by KDM2B (PRC1.1) or L3MBTL2 (PRC1.6), the first being a DNA-binding protein that specifically targets non-methylated CpG islands via its CxxC domain (Gearhart et al., 2006; Farcas et al., 2012; He et al., 2013; Wu et al., 2013; van den Boom et al., 2013; Gao et al., 2012; Qin et al., 2012). Recent publications have shown that the H2AK119ub mark itself can also independently recruit the PRC2 complex (Cooper et al., 2014; Blackledge et al., 2014; Kalb et al., 2014). In this latter scenario, the ubiquitination of H2AK119 is dependent on non-canonical PRC1 complexes.

Self-renewal of hematopoietic stem cells (HSCs) critically depends on Polycomb protein function. Homozygous deletion of *Bmi1*, encoding PCGF4 (BMI1), resulted in reduced numbers of hematopoietic progenitors and more differentiated cells, eventually leading to hematopoietic failure (van der Lugt et al., 1994). Other studies showed that BMI1 has a central regulatory role in self-renewal of HSCs by inducing symmetric cell division(s) both in mouse and human model systems (Iwama et al., 2004; Lessard and Sauvageau, 2003; Park et al., 2003; Rizo et al., 2008, 2009). Using a small hairpin RNA (shRNA) screen in human hematopoietic cells, we recently showed that many PRC1 paralog family members lack functional redundancy, suggesting that multiple PRC1 complexes exist that locate to specific target genes (van den Boom et al., 2013). In addition, murine hematopoietic cells display differentiation stage-specific expression of CBX paralogs, and a leukemogenic role for CBX7 has been suggested (Klaue et al., 2013). Similarly, PRC1 complex composition changes upon differentiation of mouse embryonic stem (mES) cells. Whereas CBX7-PRC1 is present in self-renewing mES cells and important for pluripotency, CBX7 expression is lost upon mES cell differentiation. Instead, CBX2-, CBX4- and CBX8-containing PRC1 complexes appear to regulate lineage specification (Morey et al., 2012; O'Loghlen et al., 2012). Furthermore, Morey et al. showed that PCGF2-PRC1 is required for cardiac differentiation of mES cells and that exchange of subunits enables gene repressive and activating functions of the complex that are specific for the differentiation stage (Morey et al., 2015).

Here, we investigated PRC1 paralog dependency in human acute myeloid leukemia (AML). Using an shRNA strategy in a human lentiviral MLL-AF9 leukemia model and in primary AML patient cells combined with proteome analysis, we identify the non-canonical PRC1.1 complex as an essential epigenetic regulator in leukemic cells in vitro and in vivo. Chromatin immunoprecipitation sequencing (ChIP-seq) analyses in K562 cells and primary CD34⁺ AML patient cells show that PRC1.1 binds a unique set of active genes independent of PRC2. Gene Ontology (GO) analyses of these targets reveal enrichment for genes involved in metabolism and cell-cycle regulation. Our data show that the non-canonical PRC1.1 complex is essential for leukemic stem cells and that inhibition of this complex may be beneficial for the treatment of AML.

RESULTS

Essential Role for Non-canonical PRC1.1 in Leukemic Cells

To characterize the requirement of PRC1 paralog family members for leukemic cell viability we performed an shRNA-mediated knockdown screen in our MLL-AF9 leukemic human model system (Horton et al., 2013). Cord blood (CB) CD34⁺ cells were transduced with MLL-AF9 and subsequently allowed to transform along the myeloid lineage over the course of 3–4 weeks (Figure 1A). CB MLL-AF9 (MA9)-transformed cells were subsequently transduced with pLKO.1 shRNA vectors directed against various PRC1 paralog family members. Knockdown efficiencies of shRNAs are displayed in Figure S1A. Phenotypes were evaluated in vitro followed by more detailed in vitro and in vivo analyses of selected candidates (Figure 1A). Most PRC1 paralog knockdowns displayed a mild negative effect on cumulative cell growth in sorted myeloid liquid cultures in two independent experiments (Figures 1B and S1B). However, a strongly reduced proliferation was observed upon knockdown of PCGF1, PCGF2, RING1A, and RING1B, which was also reflected by colony-forming cell (CFC) analyses where a sharp decrease of progenitor frequencies was observed (Figure 1C). We noted that CBX7 knockdown resulted in moderate phenotypes in liquid cultures while strong phenotypes were observed in CFC assays, suggesting that CBX7 is relevant for cells capable of colony formation in methylcellulose but less so for cells that sustain long-term liquid cultures. Next, we focused on the two members of the RING1 paralog family: the E3 ubiquitin ligases RING1A and RING1B. Annexin V staining revealed that both RING1A and RING1B knockdown induced apoptosis in both CB MA9 cells and K562 leukemic cells (Figures S1C and S1D) as well as in several other leukemic cell lines (data not shown). Since MLL-AF9 can give rise

(C) CFC analysis of Polycomb knockdown CB MA9 cells. Error bars represent SD.

(D) MS5 stromal co-cultures of CB MA9 cells expressing SCR, RING1A, or RING1B #1 shRNAs grown under lymphoid- and myeloid-permissive conditions. Arrows indicate time of replating.

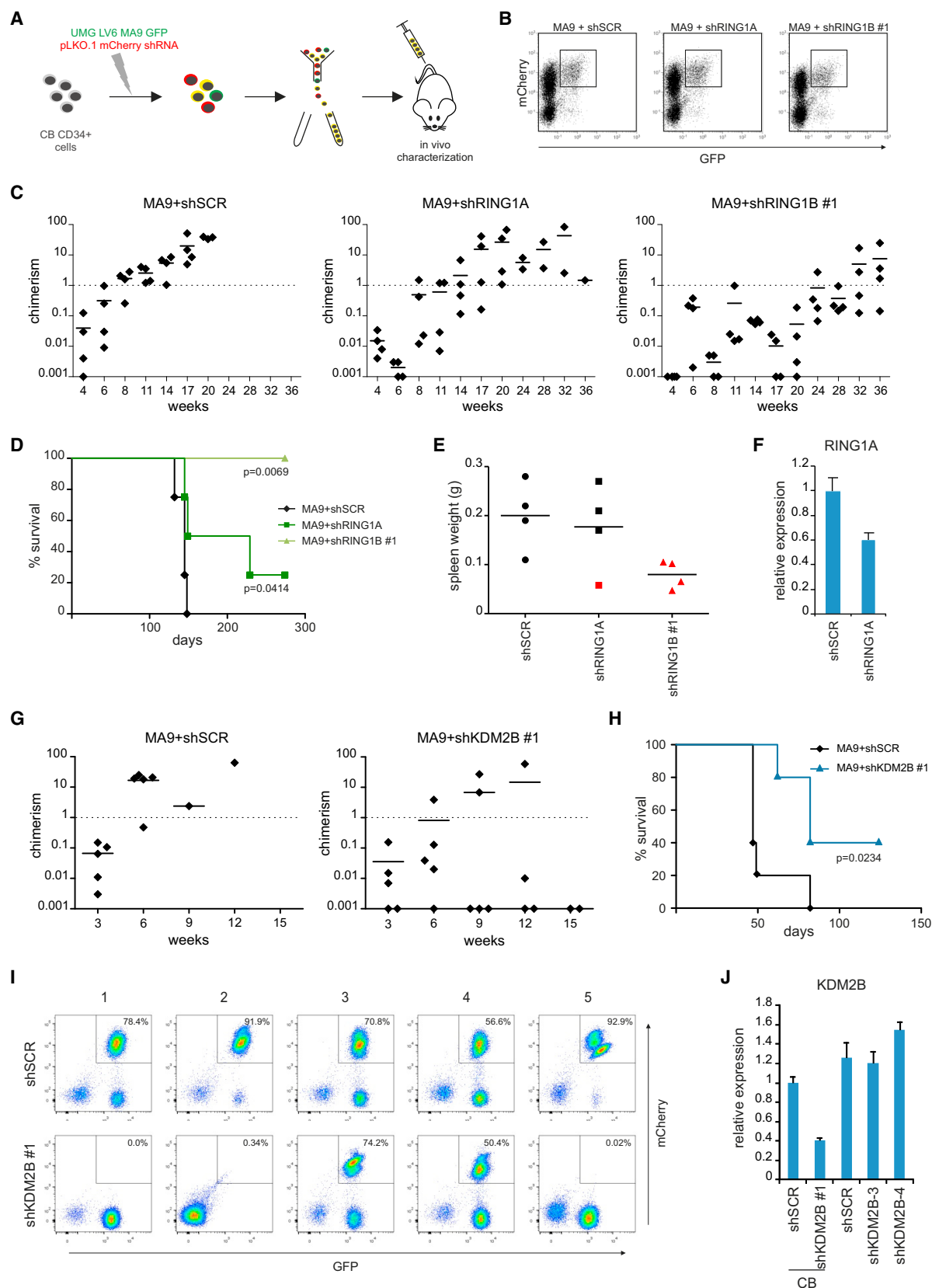
(E) Canonical and non-canonical PRC1 complex members identified by LC-MS/MS in Avi-RING1A, Avi-RING1B, Avi-PCGF1, Avi-PCGF2, Avi-PCGF4, and CBX2-Avi pullouts from K562 cells. Total spectrum counts per protein corrected for expected peptides are shown.

(F) Schematic model showing that RING1A and RING1B reside in both the canonical PRC1 complex and the non-canonical PRC1.1 complex.

(G) Relative fraction of GFP⁺mCh⁺ cells in unsorted myeloid-permissive liquid cultures of CB MA9 cells expressing SCR, PCGF1, PCGF2, PCGF4, RING1B, BCOR, and KDM2B shRNAs. Error bars represent SD.

(H) Relative fraction of GFP⁺mCh⁺ CB MA9 cells as in panel G expressing SCR, PCGF1, PCGF4, RYBP, CBX2 and KDM2B shRNAs. Error bars represent SD.

(I) CFC analysis of CB MA9 cells expressing SCR, RING1B, BCOR or KDM2B shRNAs. Error bars represent SD.



(legend on next page)

to both myeloid leukemia (AML) and lymphoid leukemia (acute lymphoblastic leukemia [ALL]), in particular in pediatric patients, we tested whether CB MA9 cells grown under lymphoid-permissive conditions were also sensitive to RING1A or RING1B knockdown. CB CD34⁺ cells were co-transduced with MLL-AF9 (GFP) and pLKO.1 mCherry (mCh) shRNA vectors, and unsorted MS5-driven bone marrow (BM) stromal cocultures under myeloid- or lymphoid-permissive conditions were initiated (Figure 1D). Next, the percentage of GFP⁺mCh⁺ cells within the total fraction of GFP⁺ cells was measured over the course of the experiment. While in the MA9/shSCR control group the GFP⁺mCh⁺ fraction was relatively stable, it was rapidly reduced in the MA9/shRING1A and MA9/shRING1B groups, both under myeloid- and lymphoid-permissive conditions, suggesting that RING1A and RING1B are essential for transformation and maintenance of both myeloid and lymphoid MLL-AF9-driven leukemias.

To investigate the molecular background of RING1A and RING1B function, we identified the interactome of RING1A, RING1B, PCGF1, PCGF2, PCGF4, and CBX2. K562 cells were transduced with vectors expressing a bicistronic transcript encoding Avi-fusion proteins and the biotin ligase BirA fused to GFP and streptavidin-mediated pull outs were performed followed by LC-MS/MS analyses (Table S1) (van den Boom et al., 2013). Figure 1E shows a summary of the interactomes of these proteins, where we focused on known canonical and non-canonical PRC1 complexes. Since the total number of potentially identifiable peptides after trypsin digestion obviously differs between proteins, total spectra counts were corrected for expected peptides based on in silico protein digests. RING1A and RING1B both co-purified many proteins that reside in canonical PRC1 complexes (PRC1.2 and PRC1.4) such as PHC, CBX, and SCML proteins (Figure 1E). In RING1B pullouts, RING1A was not detected, and in RING1A pullouts, only little RING1B was identified, in line with earlier data from our lab and others showing that RING1A and RING1B are mutually exclusive in PRC1 complexes (Maertens et al., 2009; van den Boom et al., 2013). Interestingly, we found that the non-canonical PRC1.1 complex specifically co-purified with RING1A, RING1B, and PCGF1 (Figure 1E), but not with PCGF2, PCGF4, and CBX2. This led us to speculate that the phenotypic consequence of RING1A, RING1B, and PCGF1 knockdown in MLL-AF9 leukemic cells might be a consequence of compromised PRC1.1 complex activity (Figure 1F). To more specifically address the role of the PRC1.1 complex in leukemia, we generated shRNAs directed against the PRC1.1 subunits KDM2B and

BCOR (knockdown efficiencies are shown in Figure S1A). CB MA9 cells were transduced with SCR, PCGF1, PCGF2, PCGF4, RING1B, BCOR, or KDM2B shRNAs, all with multiple independent shRNAs, and liquid cultures were initiated. Clearly, knockdown of KDM2B, BCOR, PCGF1, and RING1B induced a quick loss of the GFP⁺mCh⁺ fraction, whereas PCGF2 and PCGF4 knockdown showed a milder, though still negative phenotype (Figure 1G). Next, unsorted CB MA9 cultures were performed using two independent shRNAs directed against RYBP (a common component in various non-canonical PRC1 complexes; Gao et al., 2012; Garcia et al., 1999; Morey et al., 2013; Tavares et al., 2012), and we compared those with PCGF1, PCGF4, CBX2, and KDM2B knockdowns (Figure 1H). Interestingly, despite high knockdown efficiencies for both RYBP hairpins (Figure S1A), RYBP depletion resulted in a mild negative phenotype less severe than seen upon PCGF1 and KDM2B knockdowns. Finally, RING1B, BCOR, and KDM2B downmodulation also impaired the MLL-AF9 CFC frequency (Figure 1I). Taken together, these data show that the non-canonical PRC1.1 complex is pivotal for leukemic cell survival in vitro.

PRC1.1 Is Essential for MLL-AF9-Induced Leukemogenesis In Vivo

Next, we investigated Polycomb-dependency of leukemic cells in vivo. CB CD34⁺ cells were co-transduced with MLL-AF9 and SCR, RING1A, or RING1B shRNA vectors (Figure 2A). Next, GFP⁺mCh⁺ cells were sorted (Figure 2B), and 1×10^5 cells were injected intravenously per mouse. Peripheral blood chimerism levels of GFP⁺mCh⁺ cells were monitored by regular blood sample analysis and mice were sacrificed when chimerism levels in the blood exceeded 30%. BM, spleen, and liver analyses of sacrificed mice showed that all three organs displayed high levels of chimerism (>90%), indicative of a full-blown leukemia (Figure S2A). Leukemia development was first observed in the MA9/shSCR group. Downregulation of RING1A significantly delayed leukemia development, while knockdown of RING1B completely prevented MA9-induced leukemic transformation in vivo within the time frame of the experiment (Figures 2C and 2D). Spleen weights in MA9/shSCR leukemic mice were strongly increased compared to non-leukemic mice (Figure 2E). Despite the absence of leukemia development, MA9/shRING1B mice recurrently showed low but clearly detectable chimerism levels, which slowly increased over time (Figure 2C). Some mice transplanted with MA9/shRING1A cells did develop leukemia, but qRT-PCR analysis of BM cells from these leukemic mice showed

Figure 2. PRC1.1 Depletion Interferes with MLL-AF9 Leukemogenesis In Vivo

- Schematic overview of shRNA expression in a primary MLL-AF9 (MA9) xenograft model.
- FACS sort of MA9 (GFP) and shRNA (mCh) expressing cells at the day of injection.
- Peripheral blood chimerism of MA9/shSCR, MA9/shRING1A, or MA9/shRING1B cells over the course of the experiment.
- Kaplan-Meier survival plot of mice intravenously injected with MA9 shSCR, shRING1A, or shRING1B expressing cells (n = 4 per group). This survival plot is a representative example from two independent experiments. Statistical analysis was performed using a log-rank test.
- Spleen weights of leukemic mice (black symbols) at the day of sacrifice or non-leukemic mice (red symbols) at the end of the experiment.
- Average knockdown efficiencies of RING1A in bone marrow of leukemic mice. Error bars represent SEM.
- Peripheral blood chimerism of MA9/shSCR and MA9/shKDM2B cells over the course of the experiment.
- Kaplan-Meier survival plot of mice intravenously injected with MA9/shSCR or MA9/shKDM2B expressing cells (n = 5 per group). Statistical analysis was performed using a log-rank test.
- FACS plots showing BM analyses at the day of sacrifice of MA9/shSCR and MA9/shKDM2B mice.
- Average KDM2B knockdown efficiencies in bone marrow of SCR mice (n = 5) and two individual KDM2B knockdown mice.

that the reduction of RING1A mRNA expression levels was considerably less compared to knockdown efficiencies directly after transduction (Figure 2F). These data suggest that only clones with a relatively mild RING1A knockdown can persist, while clones with a strong RING1A knockdown do not expand or only slowly expand in vivo. In accordance with previous studies (Horton et al., 2013), leukemic mice mostly developed CD19⁺ lymphoid leukemias (ALL), and small co-existing CD33⁺/CD19[−] myeloid clones were observed only in some mice (Figure S2B).

Next, we selectively interfered with non-canonical PRC1.1 function by knocking down KDM2B. Here, an MLL-AF9 secondary transplantation model was used where leukemic cells were harvested from mice that developed a full-blown lymphoid leukemia after transplantation of MA9-transduced CD34⁺ CB cells. Subsequently, these cells were transduced with SCR and KDM2B shRNA vectors, GFP⁺mCh⁺ cells were sorted and 5×10^5 cells were intravenously injected per mouse ($n = 5$). Peripheral blood analyses showed that MA9/shSCR mice quickly developed high chimerism levels, whereas MA9/shKDM2B mice displayed a slower increase in chimerism and sometimes lost chimerism at later stages of the experiment (Figure 2G). Survival analysis showed that MA9/shKDM2B mice have a significantly delayed onset of leukemia compared to MA9/shSCR controls (Figure 2H). Importantly, the MA9/shKDM2B mice that did develop leukemia either only showed chimerism of single GFP⁺ MA9 cells (Figure 2I; likely due to sort impurities) or did not show knockdown of KDM2B (Figure 2J; KDM2B-3 and KDM2B-4).

Altered Expression of Polycomb Proteins in AML

Given that the PRC1.1 complex was of vital importance for leukemic cells, we hypothesized that the expression of its components might be deregulated in primary leukemic patient samples. Previously, we performed transcriptome studies in AML CD34⁺ cells ($n = 60$) and normal BM CD34⁺ cells ($n = 40$) (de Jonge et al., 2011). Here, we investigated which PRC2, PRC1, or PRC1.1 complex partners were significantly differentially expressed between AML CD34⁺ and normal BM CD34⁺ cells. Among others, the PRC1.1 components BCOR, PCGF1, and RING1A were significantly upregulated in AML CD34⁺ cells (Figure S2C; Table S2). Similarly, HemaExplorer datasets (<http://servers.binf.ku.dk/hemaexplorer/>) also showed that PRC1.1 members were significantly upregulated compared to normal HSC/progenitor fractions (Figure S2D; Table S2). In contrast, the expression of PRC2 complex members EZH2 and EED was significantly lower in AML CD34⁺ cells, whereas EZH1 showed increased expression.

PRC1.1 Is Required for Primary Patient AML Cell Growth In Vitro and In Vivo

Given that the PRC1.1 complex was essential for MLL-AF9-transformed cells and its expression was increased in primary AML patient cells, we investigated the functional requirement of PRC1.1 in primary samples (patient details are provided in Table S2). Primary AML patient CD34⁺ cells were transduced with SCR, RING1A, RING1B, or KDM2B shRNAs, and unsorted MS5 stromal co-cultures were initiated (Figures 3A and S3A). Knock-

down of KDM2B led to a quick loss of mCh⁺ cells over time compared to SCR control cultures, whereas shRING1B-expressing cells were lost as well but at lower rates (Figure 3B). Next, we performed co-cultures using CD34⁺ AML cells (two patients) transduced with SCR, PCGF1, PCGF2, PCGF4, RING1A, RING1B, BCOR, or KDM2B shRNAs (Figures 3B and S3B). In both AMLs, mCh⁺ cells were quickly lost upon knockdown of PRC1.1 components like KDM2B, BCOR, PCGF1, or RING1B. Slightly milder phenotypes were observed upon depletion of PCGF2, PCGF4, or RING1A. Together, these data suggest that although there is some heterogeneity between individual AML patients, the non-canonical PRC1.1 complex is critically important in AML.

Next, we tested the effect of RING1A, RING1B, or KDM2B knockdown on AML development in vivo using a humanized model that is based on subcutaneous implantation of human BM-like scaffolds as reported previously (Groen et al., 2012; Gutierrez et al., 2014; P. Sontakke and J.J.S., unpublished data). Shortly, four hybrid scaffolds consisting of three 2 to 3 mm biphasic calcium phosphate (BCP) particles loaded with human mesenchymal stromal cells (MSCs) were implanted subcutaneously into NSG mice, where they formed bone and differentiated into bone marrow stromal cells, together serving as a human niche for AML leukemic stem cells. Six weeks after implantation the scaffolds were well vascularized and scaffold 1 and 3 were injected with 200,000 mCh⁺ AML cells (AML 8) expressing SCR, RING1A, RING1B, or KDM2B shRNAs (Figure 3C). Clearly, whereas all mice injected with shSCR cells developed leukemia after ~100–130 days, only one shRING1B mouse developed leukemia, but with severely delayed onset (day 188). The other shRING1B and shKDM2B mice did not develop tumors (Figure 3D). One shRING1A mouse developed leukemia, but also with longer latency compared to SCR control mice. At day 200 after intra-scaffold injection, all remaining mice were sacrificed and no signs of tumor initiation were observed (Figure 3E). Taken together, these data suggest that PRC1.1 is functionally relevant across a broad set of AML subtypes.

PRC1.1 Targets Active Genes Independent of H3K27me3

Next, we performed ChIP-seq studies to identify non-canonical PRC1.1 and canonical PRC1 target genes in leukemic cells. For this purpose, we expressed GFP fusions of RING1A, RING1B, PCGF1, PCGF2, PCGF4, and CBX2 or non-fused GFP in K562 leukemic cells and performed ChIP reactions using an α -GFP antibody. We carefully analyzed the expression levels of GFP-fusion proteins compared to endogenous protein expression. Fluorescence-activated cell sorting (FACS) analyses showed that all cell lines displayed comparable mean fluorescence intensities of GFP (Figure S4A), and western blot analyses showed that GFP-fusion proteins were expressed at levels comparable to their endogenous counterparts (Figure S4B). Furthermore, we compared our GFP-CBX2 and GFP-RING1B tracks with endogenous CBX2 and RING1B ChIP-seq datasets in K562 cells from ENCODE/Broad, which showed strong overlap in target genes, suggesting that the GFP moiety did not interfere with chromatin targeting of the proteins (Figures S4C and S4D).

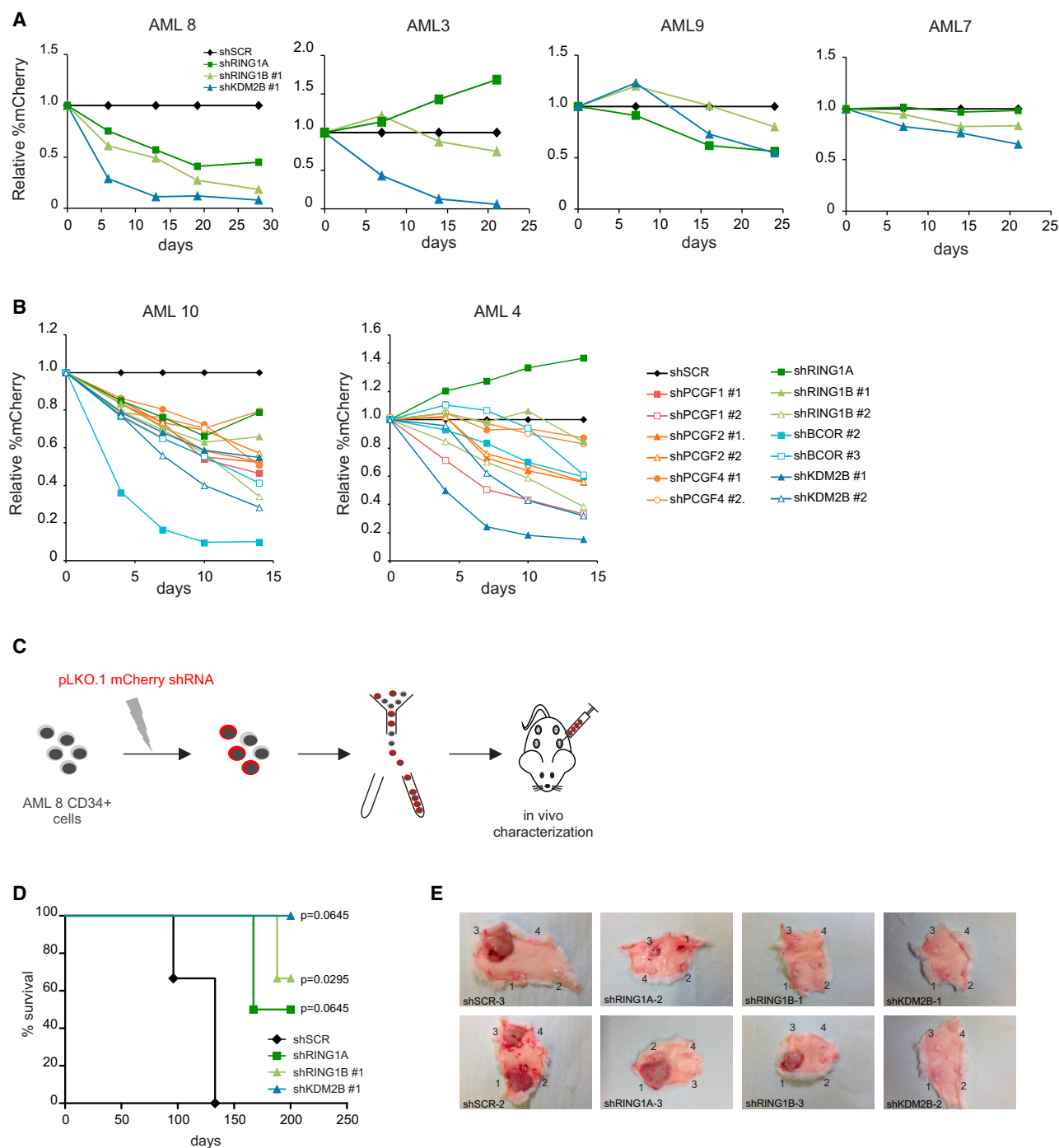


Figure 3. PRC1.1 Is Required for In Vitro Growth of Primary AML Patient Cells and Leukemogenesis In Vivo

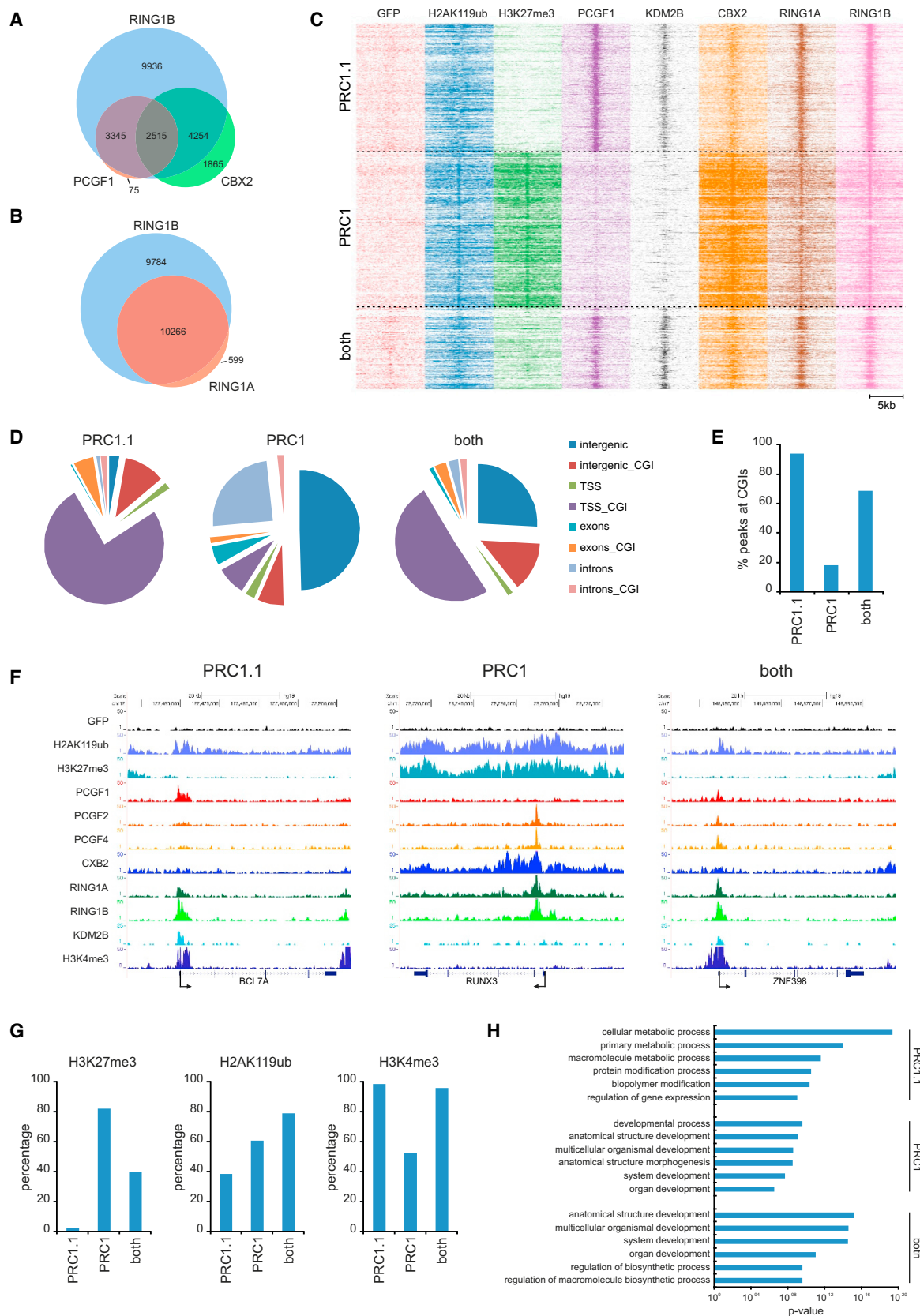
(A) Relative fraction mCh⁺ cells of primary AML patient cells from four independent patients transduced with SCR, RING1A, RING1B, or KDM2B knockdown vectors grown on a stromal cell layer.

(B) Relative fraction mCh⁺ cells as in (A), where primary AML patient cells from two independent patients were transduced with SCR and multiple PCGF1, PCGF2, PCGF4, RING1A, RING1B, BCOR, and KDM2B shRNAs.

(C) Experimental setup of our humanized niche scaffold xenograft model using primary AML patient cells transduced with pLKO.1 mCherry SCR, RING1A, RING1B, or KDM2B shRNA vectors.

(D) Kaplan-Meier survival plot of mice intra-scaffold injected with AML 8 CD34⁺ cells expressing SCR (n = 3), RING1A (n = 2), RING1B (n = 3), or KDM2B (n = 2) shRNAs. Statistical analysis was performed using a log-rank test.

(E) Pictures from skin of sacrificed mice showing vascularized scaffolds and tumors in shSCR, shRING1A, and shRING1B mice.



(legend on next page)

In addition, we also generated H3K27me3 and H2AK119ub profiles in K562 cells. Peak calling was performed, and normalized read counts were calculated for each precipitated component at each called chromosomal position. Subsequently, we identified PRC1.1 binding sites (PCGF1⁺, RING1B⁺, and CBX2⁺), PRC1 binding sites (RING1B⁺, CBX2⁺, and PCGF1⁺), and genomic regions containing both PRC1.1 and PRC1 (PCGF1⁺, RING1B⁺, and CBX2⁺; Figure 4A; Table S4). RING1A and RING1B binding sites showed a near to complete overlap (Figure 4B). Supervised clustering analysis was performed on PRC1.1 and/or PRC1 occupied loci, and heatmaps and density plots are shown in Figures 4C and S5A. Interestingly, and in contrast to PRC1, PRC1.1 binding sites were completely devoid of H3K27me3. H2AK119ub was enriched in all clusters, although distinct patterns could be observed. In addition, we performed ChIP-seq analyses using an antibody recognizing endogenous KDM2B (Figure 4C). Clearly, KDM2B was enriched at genomic loci assigned as PRC1.1 and “both” loci, but not PRC1 loci, supporting our annotation of PRC1.1 targets. Comparison of PCGF1, PCGF2, and PCGF4 showed that whereas PRC1 target genes were devoid of PCGF1, PRC1.1 target genes also showed some occupancy of PCGF2 and PCGF4 suggesting that PRC1.1 loci may, to some extent, also be co-occupied by canonical PRC1 (Figure S5B).

Genome-wide analysis of PRC1.1 and PRC1 peaks showed that PRC1.1 was mainly targeted to transcription start sites (TSSs) whereas the majority of PRC1 peaks were located in intergenic or intronic regions (Figures 4D and S5C; Table S4). Chromosomal regions harboring both PRC1 and PRC1.1 complexes generally located to TSSs or intergenic regions. In agreement with previously published data showing KDM2B-dependent PRC1.1 targeting to non-methylated CpG islands (CGIs) we observed preferential binding of PRC1.1 to CGIs (94.1%, Figure 4E) (Farcas et al., 2012; He et al., 2013; Wu et al., 2013). In contrast, PRC1 peaks did not enrich at CGIs (18.2%), and peaks targeted by both PRC1 and PRC1.1 showed intermediate enrichment for CGIs (68.9%). Genes were assigned as being regulated by PRC1.1, PRC1, or both when a peak was called within a –5 to +5 kb region relative to a TSS (GREAT; <http://bejerano.stanford.edu/great/public/html/>; Table S4; McLean et al., 2010). Thus, 2,434 PRC1.1 target genes were identified, 386 genes targeted by PRC1 and 1029 genes bound by both complexes. Representative examples of ChIP-seq profiles of PRC1.1, PRC1, and both target genes are displayed in Figure 4F. Specific comparison of these genes with our H3K27me3 and H2AK119ub ChIP-seq tracks and ENCODE/Broad K562 H3K4me3 profiles showed strong enrichment

for H2AK119ub and H3K4me3 but not H3K27me3 at PRC1.1 loci, whereas PRC1 target genes were enriched for H3K27me3, H2AK119ub, and, to a lesser extent, H3K4me3 (Figure 4G). Since PRC1.1 target genes were strongly enriched for the active chromatin mark H3K4me3 and devoid of H3K27me3, we hypothesized that PRC1.1 target genes may be actively transcribed in contrast to PRC1 target genes that are typically repressed. To investigate this, available K562 tracks (ENCODE/Broad) for H3K36me3, which enriches at actively transcribed genes throughout the gene body, and serine 5 phosphorylated active RNA polymerase II (RNAPII S5P) were analyzed. Both H3K36me3 and RNAPII S5P were strongly enriched at PRC1.1 target genes, whereas only weak enrichment was observed at PRC1 target genes (Figures S5D and S5E). GO analyses strikingly showed that PRC1.1 targeted genes involved in metabolism, whereas PRC1-bound genes were enriched for classical Polycomb-associated GO terms related to development and lineage specification (Figure 4H). Genes that were targeted by both PRC1 and PRC1.1 showed the strongest enrichment for developmental GO terms. Specific analyses for KEGG pathway-associated terms indicated that leukemia-associated pathways were enriched in the PRC1.1 as well as the “both” category of target genes.

Independent ChIP-qPCR experiments confirmed our ChIP-seq data and examples of ChIP-seq screenshots and ChIP-qPCRs are shown in Figures S6A and S6B. Strong binding of PCGF1, RING1A, and RING1B, but not PCGF2 or PCGF4, was observed around the TSSs of PRC1.1 targets LIMD2, GATA5, MYC, and PKM. These loci were also enriched for H2AK119ub and H3K4me3 marks but devoid of H3K27me3 marks. Interestingly, downmodulation of RING1A or RING1B resulted in a significant decrease in MYC expression, indicating that this locus is not repressed but likely activated by PRC1.1 (Figure S6C). In contrast, the CDKN1A locus was targeted by both canonical PRC1 and non-canonical PRC1.1 (Figures S6A and S6B) and knockdown of RING1A/B resulted in a significant increase in p21 expression, showing Polycomb repression of this locus (Figure S6C). Taken together, these data show that PRC1.1 regulates active genes involved in metabolism and cell cycle that are devoid of PRC2 activity.

Identification of Non-canonical PRC1.1 Targets in Primary AML Patient Cells

Next, we identified PRC1.1 target genes in primary CD34⁺ AML cells derived from six independent AML patients (patient details are provided in Table S3). ChIP-seq was performed using antibodies recognizing endogenous KDM2B, H2AK119ub,

Figure 4. Non-canonical PRC1.1 and PRC1 Target Unique Sets of Genes Involved in Specific Pathways

- (A) Venn diagram showing overlap of RING1B, PCGF1, and CBX2 called peaks.
- (B) Venn diagram displaying overlap of RING1A and RING1B called peaks.
- (C) ChIP-seq heatmap of peaks and surrounding regions (–5 to +5 kb) targeted by PRC1.1 (n = 3,327), PRC1 (n = 4,016), or both (n = 2,122).
- (D) Localization analysis of identified PRC1.1, PRC1, and “both” peaks across the genome. TSS, transcription start site; CGI, CpG island.
- (E) Percentage of peaks targeted by PRC1.1, PRC1, or both that are localized to CGIs.
- (F) Characteristic examples of genes targeted by PRC1.1, PRC1, or both complexes at the transcription start site (TSS).
- (G) Percentage of genes targeted by PRC1.1, PRC1, or both based on occupancy in a –5 kb to +5 kb window surrounding the TSS, which enrich for H3K27me3, H2AK119ub, or H3K4me3.
- (H) Gene Ontology (GO) analysis of genes targeted by PRC1.1, PRC1, or both.

H3K27me3, and H3K4me3. Subsequently, three categories of target genes were defined: PRC1.1 (KDM2B⁺, H2AK119ub⁺, and H3K27me3⁻), PRC1 (KDM2B⁻, H2AK119ub⁺, and H3K27me3⁺), or genes targeted by both complexes that were positive for all three marks (Figure 5A; Table S4). Heatmaps of all annotated peak regions (−5 to +5 kb) in all AMLs are shown in Figure 5B. Similar to K562 cells, genome-wide peak localization analyses showed that PRC1.1 preferentially localized to CGI-containing TSSs, whereas the majority of PRC1 bound loci localized to intergenic regions (Figure 5C). Furthermore, PRC1.1 peaks were strongly enriched for H3K4me3 (~90%) across all AML samples, whereas PRC1-specific targets showed a much lower number of peaks with H3K4me3 (~30%; Figures 5B and 5D). Genomic regions targeted by both PRC1 and PRC1.1 were also highly enriched for H3K4me3 (~98%). Figure 5E shows examples of ChIP-seq profiles of PRC1.1, PRC1, or both target genes. Similar to K562 cells, PRC1.1 was found to target the MYC and PKM genes whereas CDKN1A was targeted by both PRC1.1 and PRC1. Next, we performed independent ChIP-qPCR experiments on AML2 and AML3 and analyzed H3K27me3, H2AK119ub, H3K4me3, KDM2B, and PCGF4 occupancy at PRC1.1, PRC1, and both loci (Figure 6A). Similar to our ChIP-seq data, we observed that PRC1.1 targets were enriched for H2AK119ub, H3K4me3, and KDM2B, but not H3K27me3. In contrast, PRC1 targets showed high levels of H3K27me3 and H2AK119ub but low levels of H3K4me3 and KDM2B. Genes targeted by both complexes were enriched for H3K27me3, H2AK119ub, H3K4me3, and KDM2B. PCGF4 showed the strongest enrichment at PRC1 target genes but was also observed at some PRC1.1 target genes. GO analyses showed that PRC1.1 target genes were enriched for metabolic processes, chromatin organization, and cell cycle, whereas the PRC1-specific and both targets were highly enriched for developmental GO terms (Figure 6B; Table S5). Finally, we also performed ChIP-seq analysis on CD34⁺ cells derived from mobilized peripheral blood (PB CD34⁺). PRC1.1, PRC1, and both target genes were annotated in this sample (Figure 6C), and we tested the overlap of PRC1.1 target genes between the AML samples and control PB (Figure 6D). Thus, common PRC1.1 targets were identified, as were targets that were specific for either AML CD34⁺ cells or PB CD34⁺ cells (Figure 6D; Table S6).

DISCUSSION

Our data provided here demonstrate that leukemic cells from AML patients are critically dependent on a functional non-canonical PRC1.1 complex. Proteomics studies in leukemic cells revealed strong interactions between the RING1A/B ubiquitin ligases and non-canonical PRC1.1 proteins like KDM2B, PCGF1, and BCOR(L1). Knockdown of PRC1.1 subunits strongly impaired leukemic cell growth in vitro. PRC1.1 complex partners are frequently overexpressed in human AML patients, and using our in vivo MLL-AF9 and primary AML patient humanized niche xenograft models, we could demonstrate that leukemia initiation and maintenance both required the presence of a functional PRC1.1 complex. Finally, we observed that PRC1.1 targets a large set of active genes involved in metabolism and cell cycle in primary AML patient cells independent of H3K27me3.

A role for PRC1.1 in leukemic transformation and maintenance arose from our expression data showing upregulation of various members of the PRC1.1 complex in AML CD34⁺ cells versus normal BM CD34⁺ cells (de Jonge et al., 2011). Therefore, we hypothesize that increased PRC1.1 expression may act as an oncogenic hit in the process of leukemogenesis. In line with this idea, overexpression of murine KDM2B induces transformation of mouse BM cells and KDM2B knockdown conversely abrogates Hoxa9/Meis1-induced leukemogenesis (He et al., 2011). Interestingly, KDM2B was also overexpressed in human pancreatic ductal adenocarcinoma cells, and KDM2B collaborated with mutant KRAS to induce pancreatic tumors in mouse models (Tzatsos et al., 2013). Similarly, increased abundance of the PRC1.1 complex in human leukemic cells may act as a primary or secondary oncogenic hit.

The severe negative phenotype upon downregulation of PRC1.1 members in primary MLL-AF9 cells is in contrast with the milder phenotype observed upon knockdown of canonical PRC1 complex members like PCGF4 and CBX2. In contrast, normal CB CD34⁺ cells critically depend on a functional PRC1 complex and display strong sensitivity to CBX2 knockdown (van den Boom et al., 2013). These data suggest that PRC1 paralog dependency in normal human hematopoietic stem/progenitor cells versus leukemic cells in AML is quite distinct. The mild phenotype of PCGF4 knockdown resembles the observation that MLL-AF9-induced leukemic transformation of mouse BM cells is independent of PCGF4/BMI1, and HOXA9 may replace PCGF4/BMI1 as a repressor of the CDKN2A locus (Smith et al., 2011). Previously, Tan and colleagues reported that MLL-AF9-induced leukemogenesis depends on CBX8 in a PRC1-independent manner and suggested a co-activating role for CBX8 on MLL-AF9 target genes (Tan et al., 2011). Similarly, we found that CBX8 knockdown reduced cell proliferation and colony formation in MLL-AF9 liquid cultures and CFC analyses. In contrast to our study, knockdown of RING1B did not affect MLL-AF9-dependent cell growth in their model system, at least not in relatively short in vitro assays in which cells were analyzed for 5–10 days (Tan et al., 2011). It is currently not clear which mechanisms might underlie these different observations, but it is possible that PRC1 paralog dependency differs between human models and mouse models driven by leukemic granulocyte-macrophage progenitors.

Although knockdown of KDM2B, PCGF1, and BCOR strongly impaired MLL-AF9-induced leukemogenesis, we unexpectedly observed that downregulation of RYBP, an integral part of non-canonical PRC1 complexes, resulted in a rather mild negative phenotype in CB MLL-AF9 cells. An explanation for this phenotype could be that RYBP is replaced by its homolog YAF2, in line with previous data showing that YAF2 and RYBP can reside in variant PRC complexes in a mutually exclusive manner (Gao et al., 2012).

Using a ChIP-seq approach in K562 leukemic cells and primary CD34⁺ AML patient cells, we identified genes that are targeted by PRC1.1 and/or PRC1. In line with previous studies in mouse embryonic stem cells, we find that PRC1.1 preferentially targets CGI-containing TSSs (Farcas et al., 2012; He et al., 2013; Wu et al., 2013). Where these studies showed that PRC1.1 often

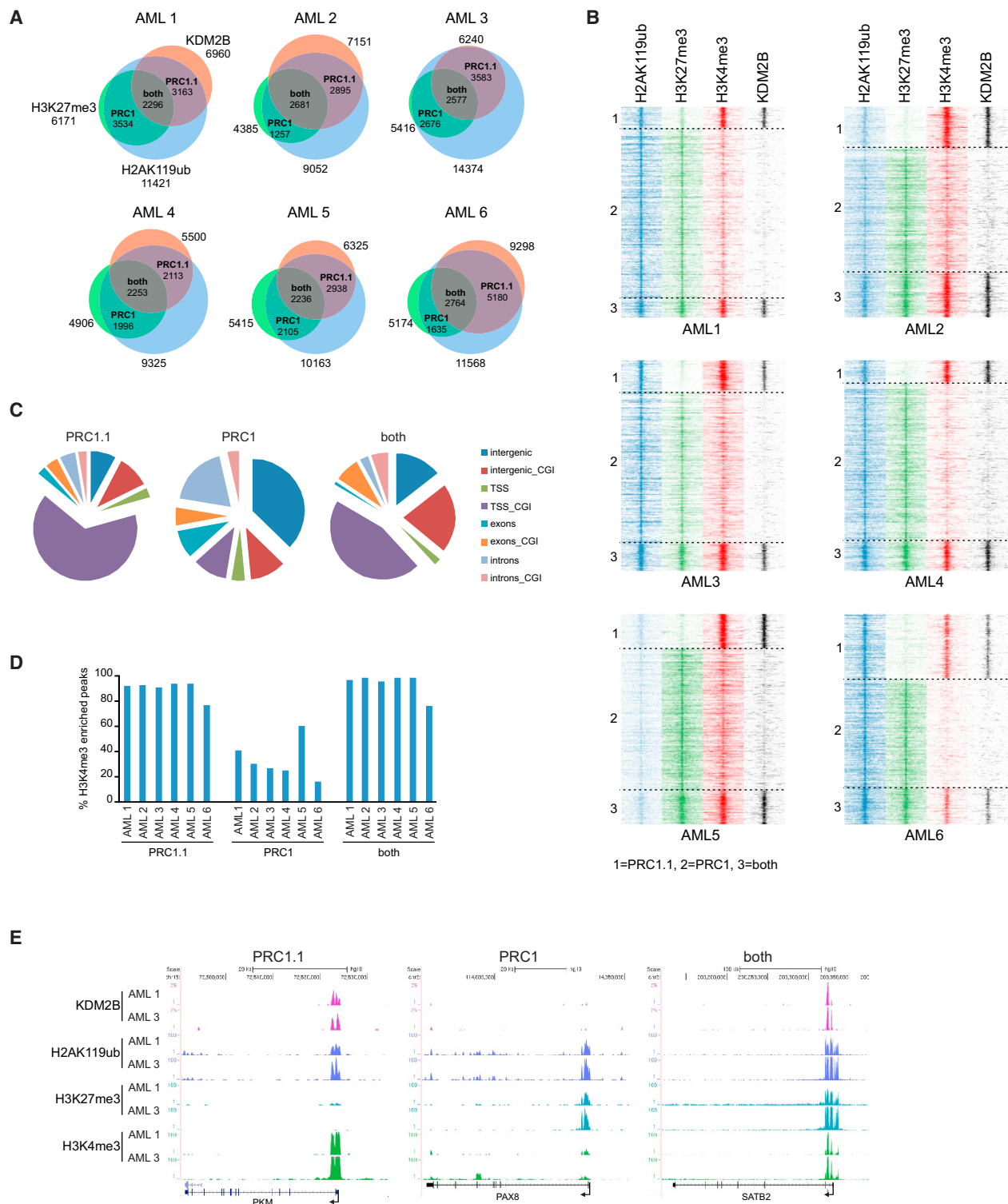


Figure 5. Distinct Targeting of Non-canonical PRC1.1 and PRC1 in Primary CD34⁺ AML Patient Cells

(A) Venn diagrams showing overlap of genes targeted by KDM2B, H2AK119ub, and H3K27me3 in six independent AML patient samples. (B) ChIP-seq heatmap of peaks (–5 to +5 kb) targeted by PRC1.1, PRC1, or both in all analyzed AML samples. (C) Chromosomal localization of peaks enriched for PRC1.1, PRC1, or both complexes. The average of all six AML samples is shown. (D) Percentage of H3K4me3-enriched peaks targeted by PRC1.1, PRC1, or both complexes in all measured primary AML patient samples. (E) Representative examples of genes targeted by PRC1.1 and/or PRC1 in two independent AMLs.

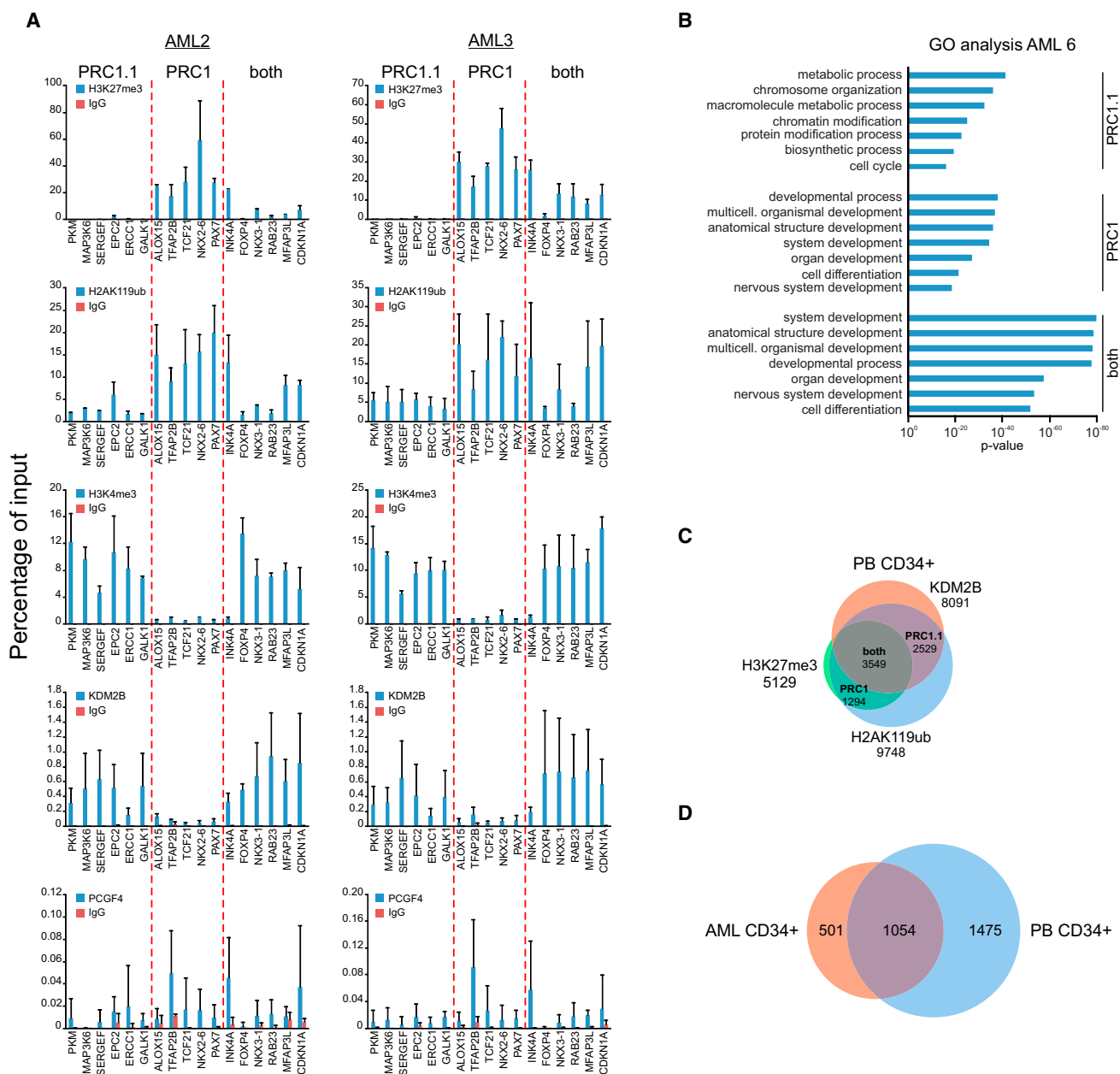


Figure 6. Specific PRC1.1 Targeting in AML and Normal PB CD34⁺ Cells

(A) ChIP-qPCR on PRC1.1, PRC1, and both target genes using antibodies directed against H3K27me3, H2AK119ub, H3K4me3, KDM2B, and PCGF4.

(B) GO analyses of gene sets targeted by PRC1.1, PRC1, or both complexes (AML6).

(C) Venn diagram showing overlap of genes targeted by KDM2B, H2AK119ub, and H3K27me3 in normal PB CD34⁺ cells.

(D) Overlap in non-canonical PRC1.1 targeted genes in AML CD34⁺ cells (we considered a gene a PRC1.1 target gene if it was found in five out of six AMLs) compared to normal PB CD34⁺ cells.

co-represses genes together with canonical PRC1 and PRC2 complexes, we observe a large fraction of genes that is preferentially targeted by PRC1.1 and enriched for H2AK119ub but devoid of H3K27me3 (Farcas et al., 2012; He et al., 2013; Wu et al., 2013). We do find some binding of PCGF2/4 at PRC1.1 sites suggesting that canonical PRC1 may also bind these loci, though with lower efficiency than PRC1.1. These data suggest

that PRC1.1 can target chromatin independently of PRC2, in line with recent data that PRC1.1 can act as an initiating complex in Polycomb-mediated silencing (Cooper et al., 2014; Blackledge et al., 2014; Kalb et al., 2014). In contrast, PRC1 target genes are strongly enriched for H3K27me3, and a category of genes targeted by both PRC1 and PRC1.1 display an intermediate situation where H3K27me3 is found but to a lesser extent

compared to exclusive PRC1 gene targets. Interestingly, Farcas and colleagues make note of low-magnitude RING1B binding sites in mES cells, which are lost upon either RING1B depletion or KDM2B knockdown and only infrequently coincide with PRC2 (Farcas et al., 2012). These sites may be similar to the PRC1.1 target genes that we identified, although we observed a strong enrichment for PRC1.1 complex members rather than weak binding. Farcas and colleagues suggested that these genes are targeted to make them susceptible to Polycomb-mediated silencing. We hypothesize that in leukemic cells, PRC1.1 might specifically regulate the activity of its target genes. In line with this idea, PRC1.1 bound genes displayed transcriptionally active chromatin profiles that were strongly enriched for H3K4me3, H3K36me3 and active RNA polymerase II. Furthermore, the expression of the PRC1.1 target gene MYC was increased upon RING1A/B knockdown, suggesting an activating role for the PRC1.1 complex. RING1B may play a role in recruitment of RNA polymerase II as recently suggested by Frangini and colleagues, who showed that RING1B, together with Aurora B kinase, regulates active genes in resting B and T cells (Frangini et al., 2013). Interestingly, a recent study shows that KDM2B binding to non-methylated CGIs prevents CpG methylation at these sites (Boulard et al., 2015). Although not addressed in our current work, PRC1.1 may prevent CGI hypermethylation at target genes, thereby maintaining their transcriptional activity.

We compared non-canonical PRC1.1 target genes in AML CD34⁺ samples with normal PB CD34⁺ samples, and we observed that besides AML-specific and normal PB-specific loci, a considerable overlap exists, suggesting that these PRC1.1 genes are controlled by non-canonical signaling in both normal and leukemic cells. Future studies will be aimed at further unraveling similarities and differences between normal and leukemic cells, but what is clear now is that PRC1.1 mostly targeted genes involved in metabolism, whereas canonical PRC1/2 predominantly binds classical Polycomb target genes involved in developmental processes. Interestingly, the non-canonical RYBP-PRC1 complex was also found to target metabolic genes in mES cells (Morey et al., 2013). Here, RYBP-PRC1 targets were annotated by the presence of RING1B, RYBP, and H2AK119ub, but not CBX7. Since RING1B and RYBP are also PRC1.1 subunits, part of these enriched regions may in fact be PRC1.1 target genes. In addition, in human pancreatic ductal adenocarcinoma cells it was also found that KDM2B targets a large group of metabolic genes independent of EZH2 (Tzatsos et al., 2013). Furthermore, Brookes and colleagues previously identified a set of active PRC loci that were enriched for metabolic genes as well (Brookes et al., 2012). Taken together, we suggest that the non-canonical PRC1.1 complex targets a variety of active genes involved in metabolism independently of H3K27me3.

These metabolic PRC1.1 target genes include enzymes functioning in the glycolytic pathway like pyruvate kinase (PKM) and lactate dehydrogenase (LDHA). KDM2B recently was suggested to positively regulate the glycolytic pathway (Yu et al., 2015). Furthermore, the Scadden lab recently demonstrated that expression of both PKM (PKM2 splice variant) and LDHA are essential for leukemogenesis and that loss of either gene re-

sulted in delayed leukemic onset of BCR-ABL and MLL-AF9 induced leukemias in vivo (Wang et al., 2014). We hypothesize that deregulated expression of these glycolytic genes upon PRC1.1 depletion contributes to the observed phenotypes in leukemogenesis. In addition, also other cancer-related genes, such as the cell-cycle regulatory gene MYC, were controlled by PRC1.1.

Taken together, we propose that the non-canonical PRC1.1 complex is essential for leukemic transformation and that its targeting might prove an excellent way to eradicate leukemic stem cells, with the ultimate aim to prevent relapse of the disease. It will be of great interest to investigate which PRC1.1-regulated cellular pathways are essential for leukemic stem cell function and whether pharmacological inhibition of either of these pathways, or PRC1.1 itself, may prove a rigid therapy in AML.

EXPERIMENTAL PROCEDURES

In Vivo Transplantations into NSG Mice

8- to 10-week-old female NSG (NOD.Cg-Prkdcscid Il2rgtm1Wjl/SzJ) mice were purchased from the Centrale Dienst Proefdieren breeding facility within the University Medical Center Groningen. Mouse experiments were performed in accordance with national and institutional guidelines, and all experiments were approved by the Institutional Animal Care and Use Committee of the University of Groningen. Prior to transplantations, mice were sublethally irradiated with a dose of 1.0 Gy (Rizo et al., 2010). Following irradiation, mice received neomycin (3.5 g/l in drinking water) and soft food daily for 2 weeks. Mice were injected intravenously with 1×10^5 sorted MA9/shSCR, MA9/shRING1A, or MA9/shRING1B CB CD34⁺ cells. Mice were sacrificed when chimerism levels in the PB exceeded 30% and/or when mice appeared lethargic.

ChIP

ChIP was essentially performed as described previously (Frank et al., 2001). Briefly, K562 cells were transduced with the lentiviral GFP-fusion vectors encoding GFP-CBX2, PCGF1-GFP, PCGF2-GFP, PCGF4-GFP, GFP-RING1A, or GFP-RING1B. K562 cells expressing GFP fusions at relatively low levels were sorted and expanded and subsequently crosslinked. ChIP reactions were performed using the following antibodies: anti-GFP (ab290, Abcam), anti-H3K27me3 (07-449, Millipore), anti-H3K4me3 (ab8580, Abcam), anti-H2AK119ub (D27C4, Cell Signaling Technology), anti-KDM2B (ab137547, Abcam), and anti-BMI1 (AF27). ChIP efficiencies were determined by qPCR.

Additional materials and methods can be found in Supplemental Experimental Procedures.

ACCESSION NUMBERS

The accession number for the ChIP-seq data reported in this paper is GEO: GSE54580.

SUPPLEMENTAL INFORMATION

Supplemental Information includes Supplemental Experimental Procedures, six figures, and six tables and can be found with this article online at <http://dx.doi.org/10.1016/j.celrep.2015.12.034>.

AUTHOR CONTRIBUTIONS

V.v.d.B., H.M., and J.J.S. conceptualization and methodology. V.v.d.B., H.M., M.G., A.R.L., J.J., A.Z.B.-V., F.F., and J.J.S. performed experiments. V.v.d.B., H.M., E.V., and J.J.S. analyzed and interpreted data. V.v.d.B., H.M., A.M.S., H.G.S., J.H.A.M., and J.J.S. performed ChIP-seq experiments and interpreted data. R.W.J.G., H.Y., and A.C.M.M. helped to setup the scaffold in vivo mouse xenograft model. V.v.d.B., H.M., and J.J.S. wrote the manuscript.

ACKNOWLEDGMENTS

The authors thank Dr. J.J. Erich and Dr. A. van Loon and colleagues (Departments of Obstetrics, University Medical Center Groningen and Martini Hospital Groningen) for collecting cord blood and J. Dales for help with cord blood stem cell isolations. We also thank Kirin for supplying TPO and Amgen for supplying Flt-3L. We greatly appreciate the input of Dr. S. Horton and Drs. M. Carretta on establishing the MLL-AF9 models and Drs. P. Sontakke for establishing the BC-CML xenograft scaffold model. We acknowledge Prof. Dr. G. Morrone for providing MLL-AF9 lentiviral vectors and Prof. Dr. K. Helin for supplying BMI1 ChIP antibody. We would also like to thank Henk Moes, Geert Mesander, and Roelof-Jan van der Lei for help with cell sorting and Simon van Heeringen for bioinformatic support. Dr. P. Valk is acknowledged for sharing AML transcriptome data. This work is supported by grants from the Dutch Cancer Foundation (RUG 2009-4275; RUG 2014-6832; KUN 2011-4937), The Netherlands Organisation for Scientific Research (NWO-VIDI 91796312), and the European Research Council (ERC-2011-StG 281474-huLSCtargeting).

Received: October 7, 2015

Revised: November 26, 2015

Accepted: December 4, 2015

Published: December 31, 2015

REFERENCES

- Bernstein, E., Duncan, E.M., Masui, O., Gil, J., Heard, E., and Allis, C.D. (2006). Mouse polycomb proteins bind differentially to methylated histone H3 and RNA and are enriched in facultative heterochromatin. *Mol. Cell. Biol.* 26, 2560–2569.
- Blackledge, N.P., Farcas, A.M., Kondo, T., King, H.W., McGouran, J.F., Hansen, L.L., Ito, S., Cooper, S., Kondo, K., Koseki, Y., et al. (2014). Variant PRC1 complex-dependent H2A ubiquitylation drives PRC2 recruitment and polycomb domain formation. *Cell* 157, 1445–1459.
- Boulard, M., Edwards, J.R., and Bestor, T.H. (2015). FBXL10 protects Polycomb-bound genes from hypermethylation. *Nat. Genet.* 47, 479–485.
- Boyer, L.A., Plath, K., Zeitlinger, J., Brambrink, T., Medeiros, L.A., Lee, T.I., Levine, S.S., Wernig, M., Tajonar, A., Ray, M.K., et al. (2006). Polycomb complexes repress developmental regulators in murine embryonic stem cells. *Nature* 441, 349–353.
- Bracken, A.P., Dietrich, N., Pasini, D., Hansen, K.H., and Helin, K. (2006). Genome-wide mapping of Polycomb target genes unravels their roles in cell fate transitions. *Genes Dev.* 20, 1123–1136.
- Brookes, E., de Santiago, I., Hebenstreit, D., Morris, K.J., Carroll, T., Xie, S.Q., Stock, J.K., Heidemann, M., Eick, D., Nozaki, N., et al. (2012). Polycomb associates genome-wide with a specific RNA polymerase II variant, and regulates metabolic genes in ESCs. *Cell Stem Cell* 10, 157–170.
- Buchwald, G., van der Stoep, P., Weichenrieder, O., Perrakis, A., van Lohuizen, M., and Sixma, T.K. (2006). Structure and E3-ligase activity of the Ring-Ring complex of polycomb proteins Bmi1 and Ring1b. *EMBO J.* 25, 2465–2474.
- Cao, R., Wang, L., Wang, H., Xia, L., Erdjument-Bromage, H., Tempst, P., Jones, R.S., and Zhang, Y. (2002). Role of histone H3 lysine 27 methylation in Polycomb-group silencing. *Science* 298, 1039–1043.
- Cooper, S., Dienstbier, M., Hassan, R., Schermelleh, L., Sharif, J., Blackledge, N.P., De Marco, V., Elderkin, S., Koseki, H., Klose, R., et al. (2014). Targeting polycomb to pericentric heterochromatin in embryonic stem cells reveals a role for H2AK119u1 in PRC2 recruitment. *Cell Rep.* 7, 1456–1470.
- de Jonge, H.J., Woolthuis, C.M., Vos, A.Z., Mulder, A., van den Berg, E., Kluijn, P.M., van der Weide, K., de Bont, E.S., Huls, G., Vellenga, E., and Schuringa, J.J. (2011). Gene expression profiling in the leukemic stem cell-enriched CD34+ fraction identifies target genes that predict prognosis in normal karyotype AML. *Leukemia* 25, 1825–1833.
- de Napolles, M., Mermoud, J.E., Wakao, R., Tang, Y.A., Endoh, M., Appanah, R., Nesterova, T.B., Silva, J., Otte, A.P., Vidal, M., et al. (2004). Polycomb group proteins Ring1A/B link ubiquitylation of histone H2A to heritable gene silencing and X inactivation. *Dev. Cell* 7, 663–676.
- Ezhkova, E., Lien, W.H., Stokes, N., Pasoli, H.A., Silva, J.M., and Fuchs, E. (2011). EZH1 and EZH2 govern histone H3K27 trimethylation and are essential for hair follicle homeostasis and wound repair. *Genes Dev.* 25, 485–498.
- Farcas, A.M., Blackledge, N.P., Sudbery, I., Long, H.K., McGouran, J.F., Rose, N.R., Lee, S., Sims, D., Cerase, A., Sheahan, T.W., et al. (2012). KDM2B links the Polycomb Repressive Complex 1 (PRC1) to recognition of CpG islands. *eLife* 1, e00205.
- Frangini, A., Sjöberg, M., Roman-Trufero, M., Dharmalingam, G., Haberle, V., Bartke, T., Lenhard, B., Malumbres, M., Vidal, M., and Dillon, N. (2013). The aurora B kinase and the polycomb protein ring1B combine to regulate active promoters in quiescent lymphocytes. *Mol. Cell* 51, 647–661.
- Frank, S.R., Schroeder, M., Fernandez, P., Taubert, S., and Amati, B. (2001). Binding of c-Myc to chromatin mediates mitogen-induced acetylation of histone H4 and gene activation. *Genes Dev.* 15, 2069–2082.
- Gao, Z., Zhang, J., Bonasio, R., Strino, F., Sawai, A., Parisi, F., Kluger, Y., and Reinberg, D. (2012). PCGF homologs, CBX proteins, and RYBP define functionally distinct PRC1 family complexes. *Mol. Cell* 45, 344–356.
- García, E., Marcos-Gutiérrez, C., del Mar Lorente, M., Moreno, J.C., and Vidal, M. (1999). RYBP, a new repressor protein that interacts with components of the mammalian Polycomb complex, and with the transcription factor YY1. *EMBO J.* 18, 3404–3418.
- Gearhart, M.D., Corcoran, C.M., Wamstad, J.A., and Bardwell, V.J. (2006). Polycomb group and SCF ubiquitin ligases are found in a novel BCOR complex that is recruited to BCL6 targets. *Mol. Cell. Biol.* 26, 6880–6889.
- Groen, R.W., Noort, W.A., Raymakers, R.A., Prins, H.J., Aalders, L., Hofhuis, F.M., Moerer, P., van Velzen, J.F., Bloem, A.C., van Kessel, B., et al. (2012). Reconstructing the human hematopoietic niche in immunodeficient mice: opportunities for studying primary multiple myeloma. *Blood* 120, e9–e16.
- Gutierrez, A., Pan, L., Groen, R.W., Baleydi, F., Kentsis, A., Marineau, J., Grebliunaite, R., Kozakewich, E., Reed, C., Pflumio, F., et al. (2014). Phenothiazines induce PP2A-mediated apoptosis in T cell acute lymphoblastic leukemia. *J. Clin. Invest.* 124, 644–655.
- He, J., Nguyen, A.T., and Zhang, Y. (2011). KDM2b/JHDM1b, an H3K36me2-specific demethylase, is required for initiation and maintenance of acute myeloid leukemia. *Blood* 117, 3869–3880.
- He, J., Shen, L., Wan, M., Taranova, O., Wu, H., and Zhang, Y. (2013). Kdm2b maintains murine embryonic stem cell status by recruiting PRC1 complex to CpG islands of developmental genes. *Nat. Cell Biol.* 15, 373–384.
- Horton, S.J., Jaques, J., Woolthuis, C., van Dijk, J., Mesuraca, M., Huls, G., Morrone, G., Vellenga, E., and Schuringa, J.J. (2013). MLL-AF9-mediated immortalization of human hematopoietic cells along different lineages changes during ontogeny. *Leukemia* 27, 1116–1126.
- Iwama, A., Oguro, H., Negishi, M., Kato, Y., Morita, Y., Tsukui, H., Ema, H., Kamijo, T., Katoh-Fukui, Y., Koseki, H., et al. (2004). Enhanced self-renewal of hematopoietic stem cells mediated by the polycomb gene product Bmi-1. *Immunity* 21, 843–851.
- Kalb, R., Latwiel, S., Baymaz, H.I., Jansen, P.W., Müller, C.W., Vermeulen, M., and Müller, J. (2014). Histone H2A monoubiquitination promotes histone H3 methylation in Polycomb repression. *Nat. Struct. Mol. Biol.* 21, 569–571.
- Kaustov, L., Ouyang, H., Amaya, M., Lemak, A., Nady, N., Duan, S., Wasney, G.A., Li, Z., Vedadi, M., Schapira, M., et al. (2011). Recognition and specificity determinants of the human cbx chromodomains. *J. Biol. Chem.* 286, 521–529.
- Kirmizis, A., Bartley, S.M., Kuzmichev, A., Margueron, R., Reinberg, D., Green, R., and Farnham, P.J. (2004). Silencing of human polycomb target genes is associated with methylation of histone H3 Lys 27. *Genes Dev.* 18, 1592–1605.
- Klauke, K., Radulović, V., Broekhuis, M., Weersing, E., Zwart, E., Olthof, S., Ritsema, M., Bruggeman, S., Wu, X., Helin, K., et al. (2013). Polycomb Cbx family members mediate the balance between haematopoietic stem cell self-renewal and differentiation. *Nat. Cell Biol.* 15, 353–362.
- Kuzmichev, A., Nishioka, K., Erdjument-Bromage, H., Tempst, P., and Reinberg, D. (2002). Histone methyltransferase activity associated with a human

- p multiprotein complex containing the Enhancer of Zeste protein.
- Genes Dev.*
- 16, 2893–2905.
- Lee, T.I., Jenner, R.G., Boyer, L.A., Guenther, M.G., Levine, S.S., Kumar, R.M., Chevalier, B., Johnstone, S.E., Cole, M.F., Isono, K., et al. (2006). Control of developmental regulators by Polycomb in human embryonic stem cells. *Cell* 125, 301–313.
- Lessard, J., and Sauvageau, G. (2003). Bmi-1 determines the proliferative capacity of normal and leukaemic stem cells. *Nature* 423, 255–260.
- Levine, S.S., Weiss, A., Erdjument-Bromage, H., Shao, Z., Tempst, P., and Kingston, R.E. (2002). The core of the polycomb repressive complex is compositionally and functionally conserved in flies and humans. *Mol. Cell. Biol.* 22, 6070–6078.
- Maertens, G.N., El Messaoudi-Aubert, S., Racek, T., Stock, J.K., Nicholls, J., Rodriguez-Niedenführ, M., Gil, J., and Peters, G. (2009). Several distinct polycomb complexes regulate and co-localize on the INK4a tumor suppressor locus. *PLoS ONE* 4, e6380.
- McLean, C.Y., Bristor, D., Hiller, M., Clarke, S.L., Schaar, B.T., Lowe, C.B., Wenger, A.M., and Bejerano, G. (2010). GREAT improves functional interpretation of cis-regulatory regions. *Nat. Biotechnol.* 28, 495–501.
- Morey, L., Pascual, G., Cozzuto, L., Roma, G., Wutz, A., Benitah, S.A., and Di Croce, L. (2012). Nonoverlapping functions of the Polycomb group Cbx family of proteins in embryonic stem cells. *Cell Stem Cell* 10, 47–62.
- Morey, L., Aloia, L., Cozzuto, L., Benitah, S.A., and Di Croce, L. (2013). RYBP and Cbx7 define specific biological functions of polycomb complexes in mouse embryonic stem cells. *Cell Rep.* 3, 60–69.
- Morey, L., Santanach, A., Blanco, E., Aloia, L., Nora, E.P., Bruneau, B.G., and Di Croce, L. (2015). Polycomb regulates mesoderm cell fate-specification in embryonic stem cells through activation and repression mechanisms. *Cell Stem Cell* 17, 300–315.
- O’Loughlen, A., Muñoz-Cabello, A.M., Gaspar-Maia, A., Wu, H.A., Banito, A., Kunowska, N., Racek, T., Pemberton, H.N., Beolchi, P., Lavial, F., et al. (2012). MicroRNA regulation of Cbx7 mediates a switch of Polycomb orthologs during ESC differentiation. *Cell Stem Cell* 10, 33–46.
- Park, I.K., Qian, D., Kiel, M., Becker, M.W., Pihalja, M., Weissman, I.L., Morrison, S.J., and Clarke, M.F. (2003). Bmi-1 is required for maintenance of adult self-renewing haematopoietic stem cells. *Nature* 423, 302–305.
- Qin, J., Whyte, W.A., Anderssen, E., Apostolou, E., Chen, H.H., Akbarian, S., Bronson, R.T., Hochedlinger, K., Ramaswamy, S., Young, R.A., and Hock, H. (2012). The polycomb group protein L3mbtl2 assembles an atypical PRC1-family complex that is essential in pluripotent stem cells and early development. *Cell Stem Cell* 11, 319–332.
- Rizo, A., Dontje, B., Vellenga, E., de Haan, G., and Schuringa, J.J. (2008). Long-term maintenance of human hematopoietic stem/progenitor cells by expression of BMI1. *Blood* 111, 2621–2630.
- Rizo, A., Olthof, S., Han, L., Vellenga, E., de Haan, G., and Schuringa, J.J. (2009). Repression of BMI1 in normal and leukemic human CD34(+) cells impairs self-renewal and induces apoptosis. *Blood* 114, 1498–1505.
- Rizo, A., Horton, S.J., Olthof, S., Dontje, B., Ausema, A., van Os, R., van den Boom, V., Vellenga, E., de Haan, G., and Schuringa, J.J. (2010). BMI1 collaborates with BCR-ABL in leukemic transformation of human CD34+ cells. *Blood* 116, 4621–4630.
- Shen, X., Liu, Y., Hsu, Y.J., Fujiwara, Y., Kim, J., Mao, X., Yuan, G.C., and Orkin, S.H. (2008). EZH1 mediates methylation on histone H3 lysine 27 and complements EZH2 in maintaining stem cell identity and executing pluripotency. *Mol. Cell* 32, 491–502.
- Simon, J.A., and Kingston, R.E. (2013). Occupying chromatin: Polycomb mechanisms for getting to genomic targets, stopping transcriptional traffic, and staying put. *Mol. Cell* 49, 808–824.
- Smith, L.L., Yeung, J., Zeisig, B.B., Popov, N., Huijbers, I., Barnes, J., Wilson, A.J., Taskesen, E., Delwel, R., Gil, J., et al. (2011). Functional crosstalk between Bmi1 and MLL/Hoxa9 axis in establishment of normal hematopoietic and leukemic stem cells. *Cell Stem Cell* 8, 649–662.
- Tan, J., Jones, M., Koseki, H., Nakayama, M., Muntean, A.G., Maillard, I., and Hess, J.L. (2011). CBX8, a polycomb group protein, is essential for MLL-AF9-induced leukemogenesis. *Cancer Cell* 20, 563–575.
- Tavares, L., Dimitrova, E., Oxley, D., Webster, J., Poot, R., Demmers, J., Bezstarosti, K., Taylor, S., Ura, H., Koide, H., et al. (2012). RYBP-PRC1 complexes mediate H2A ubiquitylation at polycomb target sites independently of PRC2 and H3K27me3. *Cell* 148, 664–678.
- Tzatsos, A., Paskaleva, P., Ferrari, F., Deshpande, V., Stoykova, S., Contino, G., Wong, K.K., Lan, F., Trojer, P., Park, P.J., and Bardeesy, N. (2013). KDM2B promotes pancreatic cancer via Polycomb-dependent and -independent transcriptional programs. *J. Clin. Invest.* 123, 727–739.
- van den Boom, V., Rozenveld-Geugien, M., Bonardi, F., Malanga, D., van Goslga, D., Heijink, A.M., Viglietto, G., Morrone, G., Fusetti, F., Vellenga, E., and Schuringa, J.J. (2013). Nonredundant and locus-specific gene repression functions of PRC1 paralog family members in human hematopoietic stem/progenitor cells. *Blood* 121, 2452–2461.
- van der Lugt, N.M., Domen, J., Linders, K., van Roon, M., Robanus-Maandag, E., te Riele, H., van der Valk, M., Deschamps, J., Sofroniew, M., van Lohuizen, M., et al. (1994). Posterior transformation, neurological abnormalities, and severe hematopoietic defects in mice with a targeted deletion of the bmi-1 proto-oncogene. *Genes Dev.* 8, 757–769.
- Vandamme, J., Völkel, P., Rosnoblet, C., Le Faou, P., and Angrand, P.O. (2011). Interaction proteomics analysis of polycomb proteins defines distinct PRC1 complexes in mammalian cells. *Mol. Cell. Proteomics* 10, 002642.
- Wang, H., Wang, L., Erdjument-Bromage, H., Vidal, M., Tempst, P., Jones, R.S., and Zhang, Y. (2004). Role of histone H2A ubiquitination in Polycomb silencing. *Nature* 431, 873–878.
- Wang, Y.H., Israelsen, W.J., Lee, D., Yu, V.W., Jeanson, N.T., Clish, C.B., Cantley, L.C., Vander Heiden, M.G., and Scadden, D.T. (2014). Cell-state-specific metabolic dependency in hematopoiesis and leukemogenesis. *Cell* 158, 1309–1323.
- Wu, X., Johansen, J.V., and Helin, K. (2013). Fbxl10/Kdm2b recruits polycomb repressive complex 1 to CpG islands and regulates H2A ubiquitylation. *Mol. Cell* 49, 1134–1146.
- Yu, X., Wang, J., Wu, J., and Shi, Y. (2015). A systematic study of the cellular metabolic regulation of Jhdmlb in tumor cells. *Mol. Biosyst.* 11, 1867–1875.